Investigation of ellipticity and pump power in a passively mode-locked fiber laser using the nonlinear polarization rotation technique

H. Ahmad[1,*], S. I. Ooi[1], M. Z. A. Razak[2], S. R. Azzuhri[1], A. A. Jasim[1], K. Thambiratnam[1], M. F. Ismail[1], and M. A. Ismail[1]

[1]*Photonics Research Centre, University of Malaya, Kuala Lumpur, Malaysia*

[2]*Institute of Microengineering and Nanoelectronics, Research Complex, University Kebangsaan Malaysia, 43600 Bangi, Selangor, Malaysia*

**Corresponding author: harith@um.edu.my*

Received November 30, 2016; accepted February 10, 2017; posted online March 3, 2017

An elliptical initial polarization state is essential for generating mode-locked pulses using the nonlinear polarization rotation technique. In this work, the relationship between the ellipticity ranges capable of maintaining mode-locked operation against different pump power levels is investigated. An increasing pump power, in conjunction with minor adjustments to the polarization controller's quarter waveplate, results in a wider ellipticity range that can accommodate mode-locked operation. Other parameters such as noise, pulsewidth, and average output power are also observed to vary as the ellipticity changes.

OCIS codes: 140.3510, 140.4050, 060.2410, 060.4370.

doi: 10.3788/COL201715.051402.

Over the last few years, fiber lasers have become the key focus in the development of new laser applications due to their significant advantages over their solid state counterparts. The key advantages of fiber lasers include their low weight and compact size, as well as relatively lower losses and ease of alignment. These characteristics make fiber lasers a crucial component of today's optical communication, carrying terabits of information across continents.

While fiber lasers can be configured to suit multiple applications, pulsed fiber lasers in particular have recently garnered substantial attention in generating high energy pulses. These pulses serve a variety of applications, including communications, sensing, manufacturing, and medicine. Pulsing in fiber lasers can be achieved by multiple active and passive means, with the most common being *Q*-switching and mode-locking. Of the two, mode-locking is preferred for applications requiring high frequency pulses but at a lower power.

Fiber lasers can be mode locked in three ways; either actively, passively, or as a hybrid of both. Active modulation is reliable and offers tunability of various parameters, but generates a broad pulsewidth[1], and also requires bulky and expensive components. Passive modulation, on the other hand, modulates the loss and gain of the laser using saturable absorbers (SAs)[2–5] or by inducing SA action, such as nonlinear amplifying loop mirrors (NALMs)[6] and nonlinear polarization rotation (NPR)[7,8]. Pulses generated in this method have pulsewidths shorter than those generated through active means, typically in the sub-picosecond region. Another approach would be hybrid methods, which combine active and passive methods to generate self-starting mode-locked laser outputs and a shorter pulsewidth[9].

Generating mode-locked pulses using the NPR technique requires two key components; namely a polarizer and an analyzer[10]. The simplicity and versatility of the NPR technique can support a large variety of applications and devices, such as the generation of supercontinuum spectra[11,12], vector solitons[13–15], all-optical flip-flop memories[16], and also in the development and fabrication of semiconductor optical amplifiers[17]. Furthermore, the NPR allows for fast saturable absorption. Recently, Smirnov *et al.*[18] has demonstrated an all-normal-dispersion mode-locked fiber laser using the NPR technique that can support a large variety of outputs by adjusting the settings of the polarization controller (PC). Different PC settings yield different spectrum energies, durations, shapes, and widths. Oliver *et al.*[19–21] demonstrated this by measuring the output polarization state, analyzing the inter-mode beat spectrum and by determining the allowed operating regimes. In this work, the relationship between pump power levels and the ellipticity of a mode-locked fiber laser of the NPR technique is successfully demonstrated. The work shows that the higher the pump power, the wider the degree of ellipticity that can accommodate a mode-locked operation.

Figure 1 shows the schematic of the experimental setup. The laser is configured in a ring cavity. A 980 nm laser diode with a maximum power of 600 mW is used as a pump source for the laser and is connected to the 980 nm port of a 980/1550 nm wavelength division multiplexer (WDM). The common output of the WDM is connected to a commercially available 65 cm long erbium-doped fiber (EDF) with a cut-off wavelength between 870–970 nm, a numerical aperture of 0.21–0.23, and an absorption coefficient of 20 dB/m at 1531 nm. The output from the EDF is

 © 2017 Chinese Optics Letters

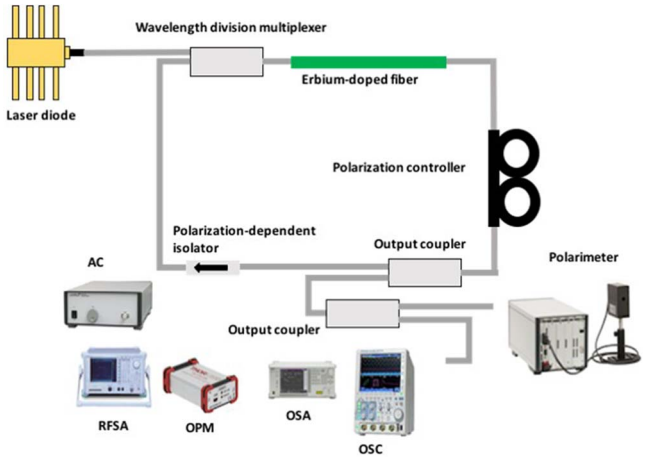

Fig. 1. Experimental setup of the proposed system.

now connected to a PC, along with a polarization dependent isolator (PDI) in the cavity. The PC and PDI act as the analyzer and polarizer for generating the desired mode-locked pulses using the NPR technique. Furthermore, the PDI has the additional function of eliminating potential reflection and backscattering from various sources inside the fiber cavity, thus ensuring the generation of the mode-locked pulses[7,22]. A 90:10 optical coupler (OC) is placed between the PC and the PDI with the common port connected to the PC's output, and the 90% port connected to the PDI's input. The OC is used to extract a portion of the signal for further analysis. Finally, the output of the PDI is connected to the 1550 nm port of the WDM, thus completing the ring cavity.

The extracted signal is further divided into two equal portions using another 50:50 OC. One portion of the signal is used to analyze the optical characteristics of the generated pulses, while the remaining portion is used to analyze the other characteristics of the pulses. Optical characterization is done using an optical spectrum analyzer (OSA) with a 0.02 nm resolution, while the measurement of the pulse characteristics is done using a photodetector coupled with an oscilloscope (OSC). Other equipment includes a polarimeter, a two-photon absorption (TPA) autocorrelator (AC), an optical power meter (OPM), and a radio frequency spectrum analyzer (RFSA) for signal-to-noise ratio (SNR) measurements.

To initiate, maintain, and optimize the desired mode-locked pulses, a PC consisting of half- and quarter-waveplates is used. This method allows for a shorter cavity. Additionally, the shorter design also allows for a higher repetition rate to be realized[23,24]. Under the right configuration and at a sufficiently high pump power, mode locking is observed starting at a pump power of about 37 mW. The total group velocity dispersion (GVD) of the system is estimated to be 0.12 ps/nm, with the single-mode fiber (SMF)-28 having a dispersion coefficient of 17 ps/nm/km at 1550 nm, and the EDF having a dispersion coefficient of −14 ps/nm/km at the same wavelength[25,26]. This indicates that the laser is operating in the soliton regime.

The relationship between the ellipticity and the pump power is taken for three conditions; e_1, e_2, and e_3. Each condition corresponds to different ellipticity degrees when observed using a polarimeter, with e_1 being the ellipticity degree at which the pulse was observed at its cleanest state, while both e_2 and e_3 are the pulses obtained at the upper and lower boundaries, just before the pulses disappear when observed using the OSC. Each condition is obtained by adjusting the quarter-waveplate only, with the upper and lower boundaries being defined as the largest and smallest angle of the PC at which mode-locked pulses can be obtained. For each condition, the pump power is adjusted between 70–110 mW in increments of 10 mW. Table 1 shows the ellipticity of all three conditions, as well as their azimuth and degree of polarization (DOP), at a predetermined pump power.

The plot of the ellipticity against the different pump power levels is given in Fig. 2. As can be seen from the figure, the increasing pump power results in the ellipticity also becoming larger for the case of e_1 and e_2. Both show an increase in the ellipticity, from between −30° to −35° at a pump power of 70 mW to between −35° to −40° at a pump power of 110 mW. The ellipticity of e_3 on the other hand decreases initially, from about −27° to around −15° as the power increases from 70 to 80 mW, before stabilizing out at a value of approximately −17° for a pump power range of between 90 to 110 mW.

This behavior can be attributed to the fact that for pulse shortening to occur in a mode-locked fiber laser, the initial polarization ellipse and phase must be properly

Table 1. Ellipticity, DOP, and Azimuth as a Function of Pump Power

Pump Power (mW)	Ellipticity, e (deg.)	DOP (%)	Azimuth (deg.)
70	e_1, −34.052	101.182	88.641
	e_2, −30.884	101.515	−76.789
	e_3, −28.298	101.795	−69.435
80	e_1, −30.624	101.152	−54.777
	e_2, −34.14	100.708	−59.948
	e_3, −17.089	100.916	−41.235
90	e_1, −34.702	100.361	−59.543
	e_2, −37.979	100.272	−72.697
	e_3, −20.214	100.82	−42.592
100	e_1, −36.193	100.396	−57.384
	e_2, −38.9	100.316	−72.155
	e_3, −19.622	100.64.	−40.7
110	e_1, −38.927	100.251	−60.201
	e_2, −41.798	100.446	−89.813
	e_3, −19.462	100.571	−37.401

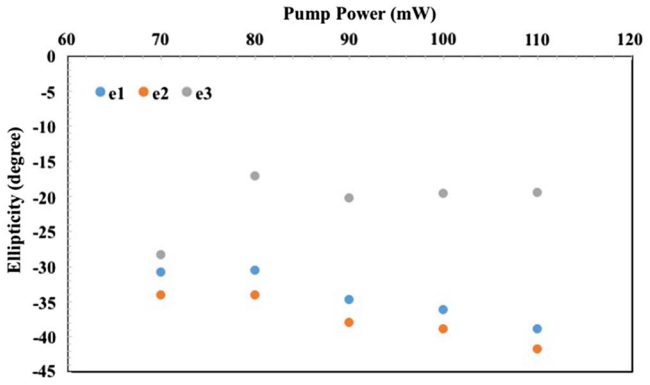

Fig. 2. Ellipticity, e_1, e_2, and e_3 at a pump power between 70–110 mW.

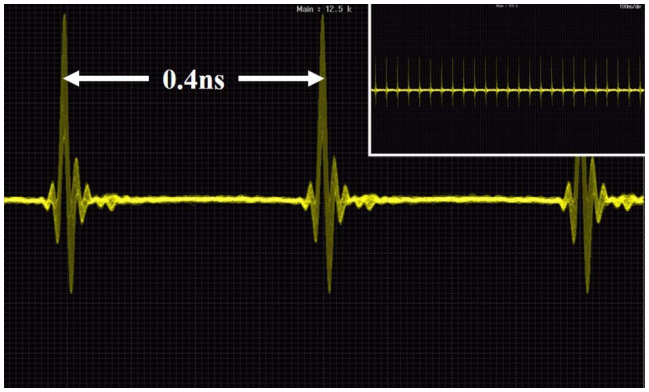

Fig. 3. Example of a mode-locked pulse from an OSC at 90 mW. The pulse train is given in the inset.

biased[8,27]. The ellipse can be resolved into right- and left-hand circular polarizations, and as the intensity of the pulse increases, due to the increasing pump power, the two components accumulate a different nonlinear phase shift relative to the intensity of the pulse. Moreover, the shift is directly related to the power difference between the two circular modes[28,29]. The result is an intensity-dependent phase shift between the coupled modes and, therefore, the nonlinear rotation of the polarization ellipse[30,31]. Feng *et al.*[32] demonstrated that the angle of rotation is proportional to the light intensity. In addition to this, and also depending on the angles and intensity, there is a region where a higher intensity pulse will experience higher losses. This, thus, creates an intensity equalizer. The balance between the inhomogeneous loss induced by the NPR and the mode competition effect of the EDF can create a stable multiwavelength oscillation with uniform power distribution between wavelengths. Moreover, the intensity of the pulses is also wavelength dependent. Therefore, since the initial polarization state of a mode-locked fiber laser using the NPR technique must be elliptical, the mode-locking operation over a wider degree of ellipticity is also realized.

The mode-locked pulse characteristics at a pump power of 90 mW is given in Table 2. It can be seen here that the ellipticity also influences the pulse width, thereby influencing the other parameters of the pulse as well. Figure 3 depicts an example of a pulse train measured using a fast photodiode connected to an OSC. The repetition rate of the laser is around 25 MHz, which corresponds to a cavity length of 8.2 m and a resulting cavity roundtrip time of 0.4 ns. The pulsewidth also changes, which can be seen in Fig. 4. Therefore, it can be ascertained that different ellipticity values yield different pulsewidths. Figure 5 shows the SNR of the pulse at a pump power of 90 mW. The SNR is measured to be 38 dB and is taken at the highest available resolution bandwidth of 300 Hz, using a 1 GHz bandwidth InGaAs photodetector connected to the RFSA. The inset of Fig. 5 shows the frequency spectrum up until 1 GHz.

The computed time–bandwidth product (TBP) deviates from an ideal value of 0.315 based on the transform limited sech2 pulse for a soliton regime. This indicates that the pulse is chirped, except when the ellipticity is −20.214°, where the transition from SA action to saturable transmitter action occurs[32]. The presence of the small peak on the left and another smaller peak on the right could be attributed to the influence of the environment towards the laser cavity. This includes air movements and also temperature variations, which would normally be the case for NPR-based experiments.

Figure 6 shows the optical spectrum taken for ellipticity values of −34.70°, −37.98°, and −20.21° for e_1, e_2, and e_3, respectively. e_1 and e_2 show an almost identical spectrum with a number of Kelly sidebands symmetrically shown on both sides. The amplitude of the sidebands varies due to the gain of the EDF and cavity construction[33]. As for the optical spectra of e_3, Kelly sidebands are more prominent, while on the other hand the middle part of the soliton spectrum becomes barely noticeable. The central wavelength shift, as can be seen in Fig. 6, is attributed to a Raman-induced frequency shift[34,35].

Table 2. Mode-locked Pulse Characteristics at 90 mW at a Different Ellipticity

Ellipticity e (deg.)	Pulsewidth (ps)	FWHM (THz)	TBP	Average Output Power (mW)	Pulse Energy (nJ)	Peak Power (W)
−34.702	0.35	0.944	0.3304	0.6194	0.0248	70.79
−37.979	0.34	1.0192	0.3465	0.6281	0.0251	73.89
−20.214	0.71	0.0325	0.0231	0.7925	0.0317	44.65

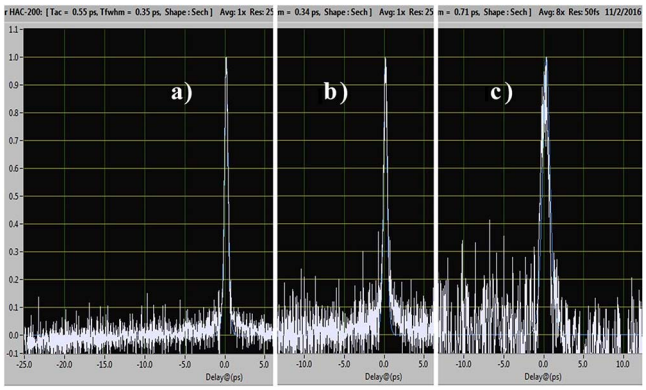

Fig. 4. Pulsewidths at 90 mW pump power at different ellipticity values (a) e_1, (b) e_2, and (c) e_3.

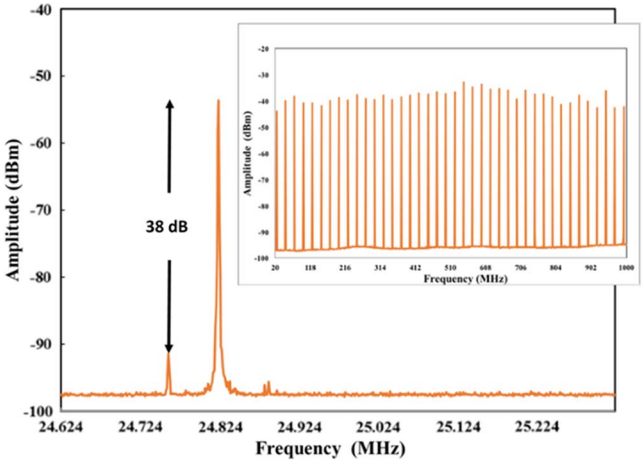

Fig. 5. SNR at 90 mW. Frequency harmonics until 1 GHz (inset).

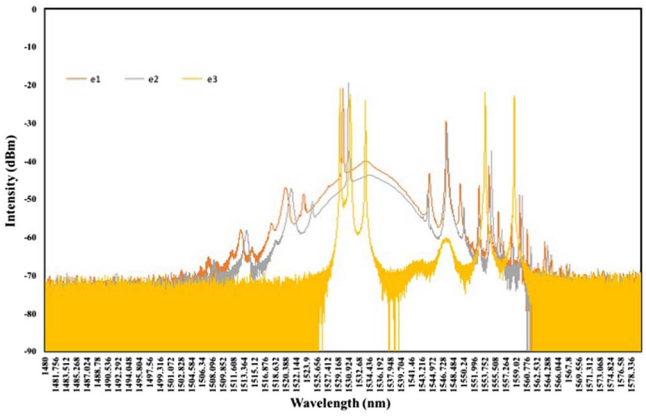

Fig. 6. Optical spectrum at 90 mW for a different ellipticity.

In conclusion, the aforementioned work successfully demonstrates the relationship between pump power levels and ellipticity in mode-locked operation. The experiment uses an NPR technique to generate a mode-locked fiber laser operating at a C-band. As the pump power is increased from 70 to 110 mW, the ellipticity range that can maintain mode-locked operation is observed to also become wider.

It can also be seen that the ellipticity influences other results, such as noise, average output power, and pulsewidth. Most importantly, it is determined that for any condition, there exists at least one ellipticity value that can produce a clean pulse against any pump power.

We thank the University of Malaya for providing funding for this research under the grants RU 010—2016, GA 010—2014 (ULUNG), and LRGS (2015) NGOD/UM/KPT.

References

1. R. Tucker, U. Koren, G. Raybon, C. Burrus, B. Miller, T. L. Koch, and G. Eisenstein, Electron. Lett. **25**, 621 (1989).
2. Q. Bao, H. Zhang, Y. Wang, Z. Ni, Y. Yan, Z. X. Shen, K. P. Loh, and D. Y. Tang, Adv. Funct. Mater. **19**, 3077 (2009).
3. U. Keller, K. J. Weingarten, F. X. Kartner, D. Kopf, B. Braun, I. D. Jung, R. Fluck, C. Honninger, N. Matuschek, and J. A. Der Au, IEEE J. Sel. Top. Quantum Electron. **2**, 435 (1996).
4. Y. Sakakibara, A. G. Rozhin, H. Kataura, Y. Achiba, and M. Tokumoto, Jpn. J. Appl. Phys. **44**, 1621 (2005).
5. F. Wang, Z. Wang, Q. Wang, F. Wang, L. Yin, K. Xu, Y. Huang, and J. He, Nanotechnology **26**, 292001 (2015).
6. M. E. Fermann, F. Haberl, M. Hofer, and H. Hochreiter, Opt. Lett. **15**, 752 (1990).
7. H. Haus, E. Ippen, and K. Tamura, IEEE J. Quantum Electron. **30**, 200 (1994).
8. A. Komarov, H. Leblond, and F. Sanchez, Phys. Rev. A **72**, 063811 (2005).
9. A. Kuznetsov, D. Kharenko, E. Podivilov, and S. Babin, Opt. Express **24**, 16280 (2016).
10. K. Tamura, H. Haus, and E. Ippen, Electron. Lett. **28**, 2226 (1992).
11. A. Proulx, J.-M. Ménard, N. Hô, J. Laniel, R. Vallée, and C. Paré, Opt. Express **11**, 3338 (2003).
12. H. Tu, Y. Liu, X. Liu, D. Turchinovich, J. Lægsgaard, and S. A. Boppart, Opt. Express **20**, 1113 (2012).
13. V. Afanasjev, Opt. Lett. **20**, 270 (1995).
14. K. Blow, N. Doran, and D. Wood, Opt. Lett. **12**, 202 (1987).
15. D. Tang, H. Zhang, L. Zhao, and X. Wu, Phys. Rev. Lett. **101**, 153904 (2008).
16. H. Dorren, D. Lenstra, Y. Liu, M. T. Hill, and G.-D. Khoe, IEEE J. Quantum Electron. **39**, 141 (2003).
17. N. Calabretta, Y. Liu, F. Huijskens, M. Hill, H. De Waardt, G. Khoe, and H. Dorren, J. Lightwave Technol. **22**, 372 (2004).
18. S. Smirnov, S. Kobtsev, S. Kukarin, and A. Ivanenko, Opt. Express **20**, 27447 (2012).
19. M. Olivier, M.-D. Gagnon, and M. Piché, Opt. Express **23**, 6738 (2015).
20. D. Radnatarov, S. Khripunov, S. Kobtsev, A. Ivanenko, and S. Kukarin, Opt. Express **21**, 20626 (2013).
21. R. Woodward and E. Kelleher, "Towards 'smart lasers': self-optimisation of an ultrafast pulse source using a genetic algorithm," arXiv:1607.05688 (2016).
22. K. Tamura, J. Jacobson, E. Ippen, H. Haus, and J. Fujimoto, Opt. Lett. **18**, 220 (1993).
23. M. Nikodem and K. Abramski, Opt. Commun. **283**, 109 (2010).
24. H. Ahmad, N. Awang, A. Latif, and S. Harun, Microwave Opt. Technol. Lett. **54**, 983 (2012).

25. I. Walmsley, L. Waxer, and C. Dorrer, Rev. Sci. Instrum. **72**, 1 (2001).
26. G. B. Pérez, T. D. J. C. Astorga, I. A. Rivera, J. I. V. Lozano, J. C. Mixcóatl, and S. M. Aguirre, in *8th IBERO American Optics Meeting/11th Latin American Meeting on Optics, Lasers, and Applications* (2013), paper 87853S.
27. L. Nelson, D. Jones, K. Tamura, H. Haus, and E. Ippen, Appl. Phys. B: Lasers Opt. **65**, 277 (1997).
28. R. Stolen, J. Botineau, and A. Ashkin, Opt. Lett. **7**, 512 (1982).
29. S. Trillo and S. Wabnitz, J. Opt. Soc. Am. B **6**, 238 (1989).
30. P. Maker, R. Terhune, and C. Savage, Phys. Rev. Lett. **12**, 507 (1964).
31. H. G. Winful, Opt. Lett. **11**, 33 (1986).
32. X. Feng, H.-Y. Tam, and P. Wai, Opt. Express **14**, 8205 (2006).
33. M. L. Dennis and I. N. Duling, IEEE J. Quantum Electron. **30**, 1469 (1994).
34. F. M. Mitschke and L. F. Mollenauer, Opt. Lett. **11**, 659 (1986).
35. J. P. Gordon, Opt. Lett. **11**, 662 (1986).